Vibrational Spectroscopy 124 (2023) 103488

Contents lists available at ScienceDirect

Vibrational Spectroscopy

journal homepage: www.elsevier.com/locate/vibspec

Raman imaging studies on the stability of Paracetamol tablets under different storage conditions

Sara Fateixa *, Otílio Mulandeza, Helena I.S. Nogueira, Tito Trindade

Department of Chemistry and CICECO-Aveiro Institute of Materials, University of Aveiro, 3810-193 Aveiro, Portugal

ARTICLE INFO

Keywords:
Raman imaging
Paracetamol
4-Aminophenol
Pharmaceutics

ABSTRACT

The applicability of Raman imaging for pharmaceutics production ranges from the characterization of pharmaceutical formulations, kinetic processes in drug delivery to the rapid detection and identification of counterfeit drugs/contaminants. Acetaminophen (Paracetamol, APAP) is an analgesic and antipyretic drug and one of the most consumed medicines worldwide. On the other hand, the compound 4-aminophenol (4-AP) is a hydrolytic product of APAP with nephrotoxicity and teratogenic effects. In this work, we have explored for the first time Raman imaging methods to characterize the main components of commercial APAP tablets (APAP-tablets) and to inquire about the potential of this optical technique to identify 4-AP in APAP tablets, which have been previously spiked with such contaminant. The laboratorial treated APAP-tablet samples were subjected to different temperature, humidity and sunlight exposure conditions, mimicking storage conditions, and then the Raman spectra and images were collected to monitor changes that might occur in those conditions. Although the lower limit of detection of 4-AP in APAP-tablets is above the minimum levels established by Pharmacopoeias (0.005 %), this research demonstrates that Raman imaging still allows the detection of small amounts of the contaminant, thus opening perspectives for exploring this technique for characterizing APAP products.

1. Introduction

The chemical stability of drugs' active pharmaceutical ingredients (APIs) is fundamental in pharmaceutical formulation quality control. This process verifies whether the product complies with the pharmacopoeia specifications, such as the World Health Organization (WHO) and European Union legislation (EU) [1]. International Organization for Standardization (ISO) 8402–1986 has defined quality as "the totality of features and characteristics of a product or service that bears its ability to satisfy stated or desired needs". The quality of the pharmaceutical formulation can be guaranteed by evaluating several drug characteristics, such as weight variation test, hardness, friability, disintegration, dissolution and assay tests [1–3]. Evaluating these parameters ensures the API quality regarding therapeutic activity's optimization and bioavailability because irregularities and poor quality of the pharmaceutical formulations can represent a series of complications for the pharmaceutical company, namely re-manufacture, loss of credibility and can compromise the operating license and product registration [4,5].

On the other hand, for consumers, the lack of quality of pharmaceutical products can cause a series of disorders or even compromise their health [6,7]. Unfortunately, chemical alterations in the pharmaceutical formulations can occur as consequence of exogenous factors, such as illegal counterfeiting of drugs for public consumption and, chemical instability of APIs due to interaction between APIs and excipients in non-optimal conditions. For example, the latter can be caused by the deterioration of packaging system (e.g. pills or capsules), due to non-favorable environmental conditions during transportation, storage and use, especially in tropical climates [3].

Exposure to certain environmental conditions of temperature, humidity, light and oxygen, for example, might affect the chemical stability of the API due to its hydrolysis, oxidation, isomerization, polymerization and photochemical degradation. Additionally, physical changes can also occur in the drug's hardness, friability, disintegration and dissolution rate, leading to changes in the bioavailability of the drug [8–12]. Several drugs have amide or ester groups in the API molecular constitution, which are prone to undergo hydrolysis in high relative humidity levels (RH) [12,13]. There is a variety of classes of drugs that can experience this alteration, which include antibiotics, anaesthetics, vitamins and barbiturates when exposed to moisture [12,13].

* Corresponding author.
E-mail address: sarafateixa@ua.pt (S. Fateixa).

https://doi.org/10.1016/j.vibspec.2022.103488
Received 22 October 2022; Received in revised form 28 November 2022; Accepted 9 December 2022
Available online 12 December 2022

Paracetamol (APAP), also called acetaminophen or N-acetyl-ρ-aminophenol, is an acetylated aromatic amide synthesized by Morse (1878) and used for the first time in medicine by Von Mering (1893) [14]. However, it was only in 1949 that it was officially introduced as a therapeutic agent [15]. Nowadays, it is accepted worldwide as an effective drug for relieving pain and fever in adults and children [16]. It is presented in several pharmaceutical formulations as a suspension, solution, tablet, or capsule [17,18]. The main product of the APAP hydrolytic degradation is 4-aminophenol (4-AP) or ρ-aminophenol [19,20]. The compound 4-AP is reported to have significant nephrotoxicity and teratogenic effects [21,22], and it has been limited to the low level of 50 ppm (0.005 % w/w) in pharmaceutical formulations by the European and US Pharmacopoeias, by employing a manual colourimetric limit test [23,24]. Other techniques have been used for determining 4-AP in APAP tablets, such as spectrophotometry,[25] high-performance liquid chromatography (HPLC) [26–28], liquid chromatography coupled with mass spectroscopy (LC/MS) [29], capillary electrophoresis [30,31], flow injection analysis [24], and micellar electrokinetic chromatography [32,33]. However, most of the procedures mentioned above are time-consuming, expensive and require specialized labour. Raman imaging and spectroscopic methods, as non-destructive and sensitive methods are valuable complementary tools for quality control for detecting and monitoring 4-AP in paracetamol tablets.

Confocal Raman microscopy (CRM) is among the alternative analytical tools that have been exploited in the last years to investigate APIs' stability and quality control, leading to new possibilities for two-dimensional characterization of samples. Recent advances in vibrational microscopy imaging [34,35], allows the acquisition of chemical images under sub-micron resolution in a reduced time for visualizing particle size and spatial distribution of APIs and excipients in specific samples, such as pills, tablets or capsules, leading to consistent fabrication of pharmaceutical products [36–39].

Recent applications of Raman mapping on pharmaceutical formulations include the composition of tablets [40,41] and the connection between composition and dissolution rate [42]. This technique can also be used in other real-world applications such as agriculture and biomass (*e.g.*, characterisation of fertilisers and soils) [43], environmental (*e.g.*, microplastics identification, water quality monitoring) [44,45], food industry (*e.g.*, food quality, pesticides detection) [46], biological and medical applications (*e.g.*, study/characterisation of cells and identification/diagnosis of diseases) [47,48], Geology [49], Arts, archaeology and palaeontology [50] and Forensic analysis (*e.g.*, fingerprints, hand-writing) [51,52].

Due to typically higher Raman scattering coefficients of APIs, as compared to common excipients, Raman imaging can detect low amounts of APIs and related substances, namely contaminants and polymorphs, by creating high resolution chemical images [53–55]. For example, Widjaja et al. have detected magnesium stearate, a minor component of pharmaceutical drug tablets, using Raman imaging and multivariate data analysis [56]. In a laboratorial prepared tablet, they have successfully acquired a Raman spectrum of magnesium stearate at a low concentration of 0.2 wt %. Šašić has reported Raman mapping coupled with chemometrics to study the spatial distribution of alprazolam in commercial Alprazolam/Xanax tablets with an alprazolam loading lower than 1 % (w/w) [57]. Marsac and co-workers have developed a method involving a two-step Raman mapping approach to investigate salt disproportionation in tablets with low drug content (5 % w/w) [58]. Our interest in the pharmaceutical areas led us to explore Raman imaging as a tool to study and characterize systems that can be used in drug delivery, cancer therapies and bone regeneration [59–62]. More recently, we have reported our research results on applying CRM as an essential tool to monitor polymorphism transition/degradation compounds [63] and hydration processes in APIs in tablets [64]. In particular, Raman imaging coupled with cluster analysis was explored to identify and monitor the polymorph transition of anhydrous carbamazepine (CBZ III; polymorph III), an anticonvulsant drug commonly used to treat epilepsy, into CBZ I (polymorph I) and iminostilbene (API degradation), in function of temperature [63] and the hydration of CBZ at the nanoscale level [64]. The spatial distribution of CBZ III in commercial tablets was also reported using Raman imaging, demonstrating the potential of this approach for quality monitoring purposes. In the latter, after seventeen days of exposure to RH 89 %, the commercial CBZ III protective coating is falling apart and the presence of CBZ DH is noticed by Raman imaging.

Here, we explore CRM to obtain the spatial distribution of the main components of commercial APAP tablets and to identify 4-AP in samples, that have been laboratorial prepared by adding such contaminant in low concentration. To the best of our knowledge, there are no Raman imaging studies for identifying 4-AP (a minor component, 0.1 % w|w) alongside major components, such as APAP in pharmaceutical formulations. Furthermore, CRM was used to gain new insights into the hydrolysis/degradation behaviour of commercial paracetamol tablets (APAP-tablets) spiked with 4-AP stored at above room temperature and humidity, demonstrating the potential of this approach for quality monitoring purposes.

2. Experimental section

2.1. Materials

Commercial paracetamol tablets (1 g of APAP) were obtained from a specific supplier which are designed as APAP-tablet for confidential reasons. Acetaminophen (APAP, purity 99 %, $C_8H_9NO_2$) and 4-aminophenol (4-AP, purity 99 %, C_6H_7NO) were purchased from Sigma-Aldrich and used as received.

2.2. Preparation of APAP-tablet containing 4-AP

The APAP-tablets were ground in a mortar with a pestle and then a certain amount of 4-AP was added and mixed with the powder, to obtain a series of APAP-tablets contaminated with 4-AP, at the following final concentrations 0.05 %, 0.1 %, 0.5 %, 1 % and 10 % (w|w in 4-AP). For each blend, three tablets with diameters of 25 mm (thickness of 2.5 mm) and 200 mg in weight have been prepared by using a hydraulic press (8 t). Tablets containing only APAP were also pressed and used as controls.

2.3. Storage conditions

APAP-tablet containing different loading of 4-AP (0.5 %, 1 % and 10 %) were studied after being submitted to different storage conditions, such as relative humidity, temperature and sunlight exposition.

2.3.1. Humidity and sunlight tests

The APAP-tablets were placed in a closed compartment either at 65 % or 86.5 % relative humidity (RH), at room temperature (22ºC), over four weeks. For RH 86.5 %, a glass of water was placed inside the closed compartment. The relative humidity and temperature were monitored using a digital humidity sensor (Hygrometer testo 608-H-1). For RH 65 % at 22ºC, some tablets were placed in a closed compartment exposed to the sunlight, while other samples were stored in the dark for 4 weeks.

2.3.2. Temperature tests

Tablets were placed in an oven at different temperatures (22ºC and 40ºC) in the dark for 4 weeks.

2.4. Confocal Raman microscopy (CRM)

Raman spectra of APAP and 4-AP were measured using a combined Raman-AFM-SNOM confocal microscope system WITec alpha300 RAS$^+$. A Nd:YAG laser operating at 532 nm with a 100x (0.9 NA) objective was used to acquire single Raman spectra in the range between 0 and 3700

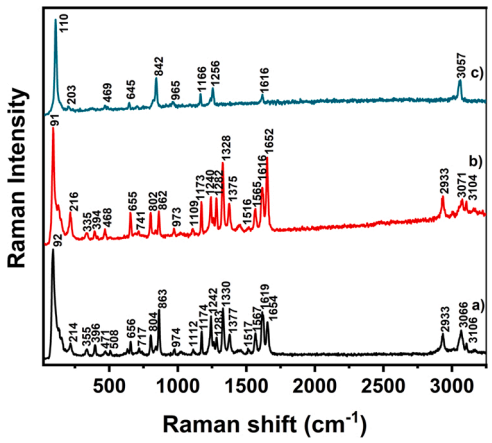

Fig. 1. Experimental Raman spectra of APAP-tablet (a), APAP powder (b), and 4-AP powder (c).

cm^{-1}. Each Raman spectrum was acquired with 10 scans, 2 s each at a power of 5 mW. The WITec microscopy has a RayShield filter providing Raman spectra measurements at extremely low wavenumbers down to below 10 rel.cm^{-1}.

Raman imaging was performed by taking several Raman spectra in a uniform grid with different areas. The integration time for each spectrum was 0.1 s for small areas (approximately 67 min) and 0.05 s for large areas (approximately 133 min) in the range between 0 and 3700 cm^{-1}. All the parameters used for each Raman image are described in Table S1 (Supporting information).

2.5. Data processing

Data acquisition and processing were performed using WITec Project 5.3^{+} software. The average Raman spectra were obtained from all data points in the Raman images. Background subtraction using the shape function (shape size: 300; noise factor: 2) was performed for all Raman spectra and images (WITec Project 5.3^{+}). All imaging data were analyzed using the command True Component Analysis (WITec Project 5.3^{+}) to create the combined Raman image. The True Component Analysis uses a basic analysis algorithm to fit the measured spectrum at each pixel as a linear combination of the reference library spectra using a least squares method [65,66]. The Raman spectra of APAP, 4-AP, stearic, and corn starch were used to build a True Component reference library. Application of the True Component linear combination model to the hyperspectral dataset resulted in a component distribution image for each library component. The intensity of each pixel in the distribution image is determined by degree of membership to a particular component by fitting the spectral response at the specific pixel with the reference library spectra. This was given an arbitrary value between 0 and 1, where a score value of 0 represents the absence of a component in a pixel and a score value of 1 demonstrates 100 % presence a component. False-colour chemical images are the overlap of the Raman images for each component (red for paracetamol, cyan for 4-aminophenol, blue for corn starch and green for stearic acid).

2.6. Fourier transform infrared- (FTIR) spectroscopy

FTIR data were acquired using a Bruker Optics Tensor 27 coupled to a horizontal attenuated total reflectance (ATR) cell, using 256 scans at a 4 cm^{-1} resolution.

3. Results and discussion

The Raman spectra of APAP-tablet and APAP powder are presented in Fig. 1a,b. APAP crystallizes in three forms (polymorphs) and occurs as an amorphous phase, among which the thermodynamically monoclinic form (type I) corresponds to the API present in commercial APAP [67–69]. The Raman spectrum (Fig. 1b) of monoclinic APAP exhibits the characteristic bands at 1240 and 1328 cm^{-1}, assigned to the stretching vibrations of the aromatic C-O and C-N groups, and three well-resolved peaks in the 1500–1700 cm^{-1} region, which are assigned to the amide carbonyl group vibrations and the aromatic hydrogens.[68,69].

The vibrational band assignments for APAP are presented in Table S2 (Supporting information). Although slight differences exist in the intensity of certain bands, the Raman spectrum of the APAP-tablet matches well with the corresponding spectrum of APAP powder. Fig. 1c also shows the Raman spectrum of a sample of pure 4-AP, a contaminant that might be formed from APAP in hydrolytic conditions. The experimental spectra shown in Fig. 1 were used as a basis to investigate the distribution of APAP over the APAP-tablets by Raman imaging.

In Fig. 2, the area marked in red corresponds to the optical microscopy image of the APAP-tablet and the corresponding combined Raman images are shown on the right panel, for consecutive decreasing areas scanned over the sample. A total of 160 000 Raman spectra (400 points x 400 lines) were collected across the entire pellet surface (13.5 mm × 13.5 mm) to generate the Raman map presented in Fig. 2B, which overall shows the presence of APAP over the tablet, i.e. a red region characterized by the Raman spectrum shown in Fig. 2I. A close inspection of a smaller area (1.35 mm × 1.35 mm) using the acquired 160 000 Raman spectra, demonstrates the presence of other ingredients with distinct Raman spectra (Fig. 2D, I). Although APAP is still observed as the main component (red colour), other spectral features are also observed probably due to excipients present, namely corn-starch (blue colour) and stearic acid (green colour) [70,71]. Hence, the spectra show the characteristic bands of starch macromolecules (Raman spectrum in blue; Fig. 2I) at 477 cm^{-1} assigned to the δ(CCC) + δ(CCO); 868 cm^{-1} assigned to the δ(CCH) + δ(COC); 941 cm^{-1} assigned to the δ(COC) + δ(COH) + ν(CO); 1127 cm^{-1} assigned to ν(CO) + ν(CC) + δ(COH); 1461 cm^{-1} assigned to the δ(CH) + δ(CH_2) + δ(COH) and 2911 cm^{-1} assigned to the ν(CH).[71] The Raman spectrum of the compound APAP (red spectrum, Fig. 2I) shows all the characteristic bands assigned to APAP powder (see table S2) [72,73]. The Raman spectrum depicted in green (Fig. 2I) is due to the presence of stearic acid, showing three characteristic bands at 2846 cm^{-1}, 2880 cm^{-1} and 2940 cm^{-1}, assigned respectively to the $\nu_{sym}(CH_2)$, $\nu_{asym}(CH_2)$ and $\nu_{sym}(CH_2)$ + 2 δ(CH_2) modes; 1442 cm^{-1} assigned to the δ(CH_2) + δ(C═O) + ν(CO) + δ(C-OH) mode; 1298 cm^{-1} assigned to the t(CH_2) mode; 1130 cm^{-1} assigned to the ν_{sym}(CC) and 1061 cm^{-1} assigned to the ν_{asym}(CC) [74].

The high-resolution Raman images (Fig. 2F, G) show the distribution of small grains of APAP (red colour) over the APAP-tablet's surface and the presence of bigger grains with about 12 μm of diameter of corn-starch (blue colour). Thus, these results show APAP homogeneously distributed in the tablet, which also contain corn-starch and stearic acid enriched regions in a lower amount. To validate the method used to produce the Raman images, single Raman spectra were collected in different regions of the APAP-tablet (red and blue regions, Fig. 2G). Fig. 2H shows two distinct Raman spectra acquired in different APAP-tablet regions, in which the presence of APAP (red spectrum, Fig. 2H) was confirmed in the red region and corn starch in the blue region (blue spectrum, Fig. 2H).

The Raman spectrum of 4-AP powder is presented in Fig. 1c, which is quite different from the APAP's Raman spectrum, thus allowing their distinction by this spectroscopic technique (Fig. 1b). Hence, the Raman spectrum of pure 4-AP shows distinctive features in the CH stretching region at 2800–3000 cm^{-1} and in the 1200–1350 cm^{-1} region of the stretching vibrations of aromatic C-O and C-N linkages. Also, in the 1500–1700 cm^{-1} region, with the disappearance of the bands set to the amide carbonyl group vibrations and at lower frequencies [75]. In particular, the low-frequency Raman band at 110 cm^{-1} can be employed as diagnosis spectroscopic features to monitor the presence of 4-AP.

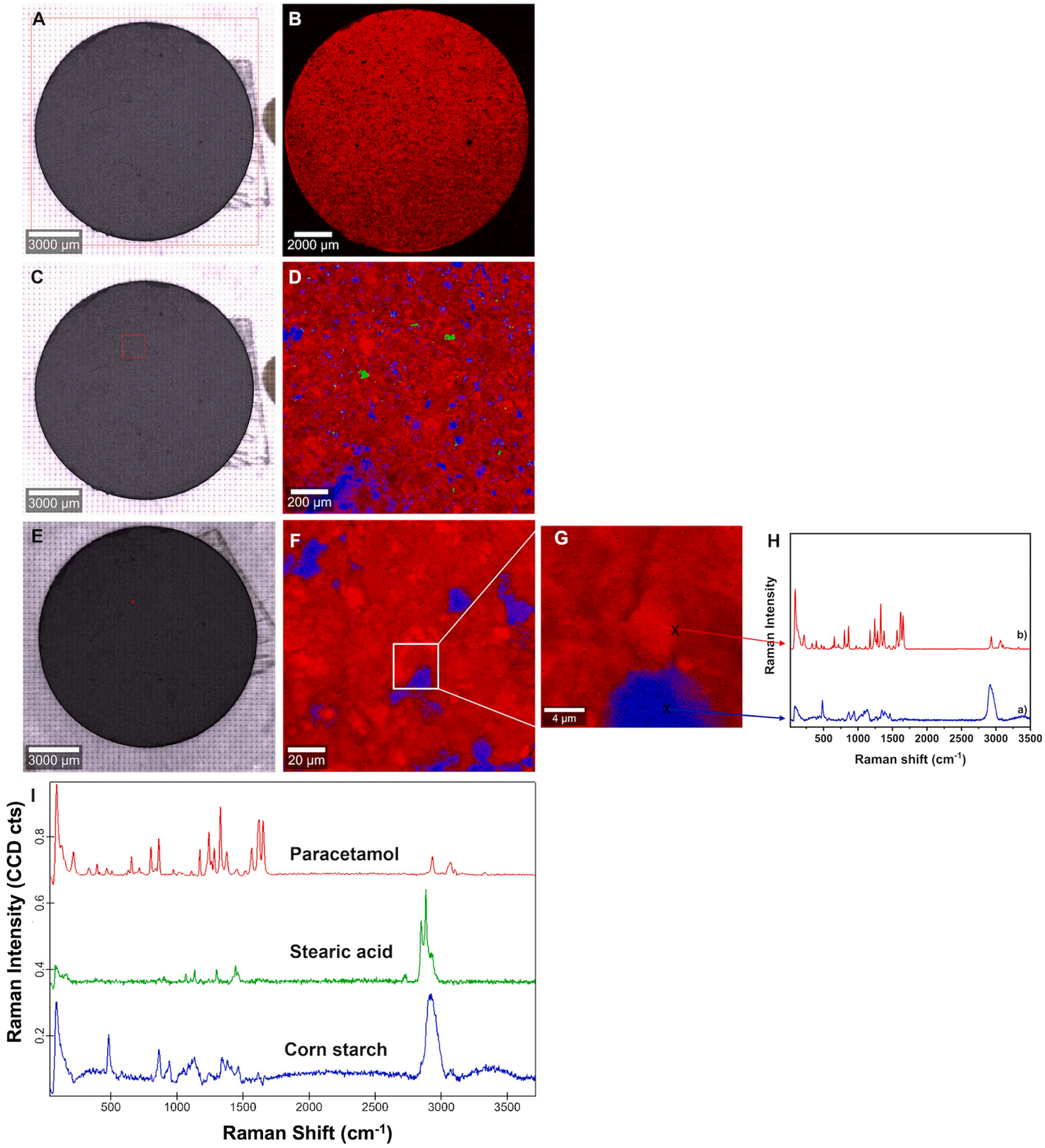

Fig. 2. Optical images of APAP-tablet with the scan area marked in red, for decreasing dimensions: 13.5 mm x 13.5 mm (A); 1.35 mm x 1.35 mm (C), and 135 µm x 135 µm (E), and the respective combined Raman image with 400 × 400 Raman spectra each image (B, D and F); High-resolution Raman image with 200 × 200 Raman spectra in a 20 µm x 20 µm area (G); (H) Single Raman spectra acquired at different regions of the Raman image identified as APAP (a) and corn starch (b); (I) Raman spectra used for the combined Raman image: corn-starch (blue), APAP (red) and stearic acid (green).

The laboratorial APAP-tablets spiked with 4-AP (10 % w|w) were analyzed by Raman imaging to investigate the distribution of the added impurity over the APAP-tablet_10 %. Fig. 3 presents the optical image of the APAP-tablet_10 % with the scanned area marked in red (A, C, E), and the combined Raman images collected for consecutive decreasing areas (B, D, F). As expected, both the APAP and 4-AP components are observed on the surface of the APAP-tablet_10 %, for the scanned larger area (13.5 mm × 13.5 mm; 160 000 Raman spectra), as presented in Fig. 3A. The Raman image (Fig. 3B) shows two distinct chemical components in the whole tablet: APAP (red spectrum; Figs. 3H) and 4-AP (cyan spectrum; Fig. 3H).

As the scanned area decreased, the corn-starch grains and stearic acid were also detected (Fig. 3D, F) (blue spectrum_corn starch; green spectrum_stearic acid, Fig. 3G);.

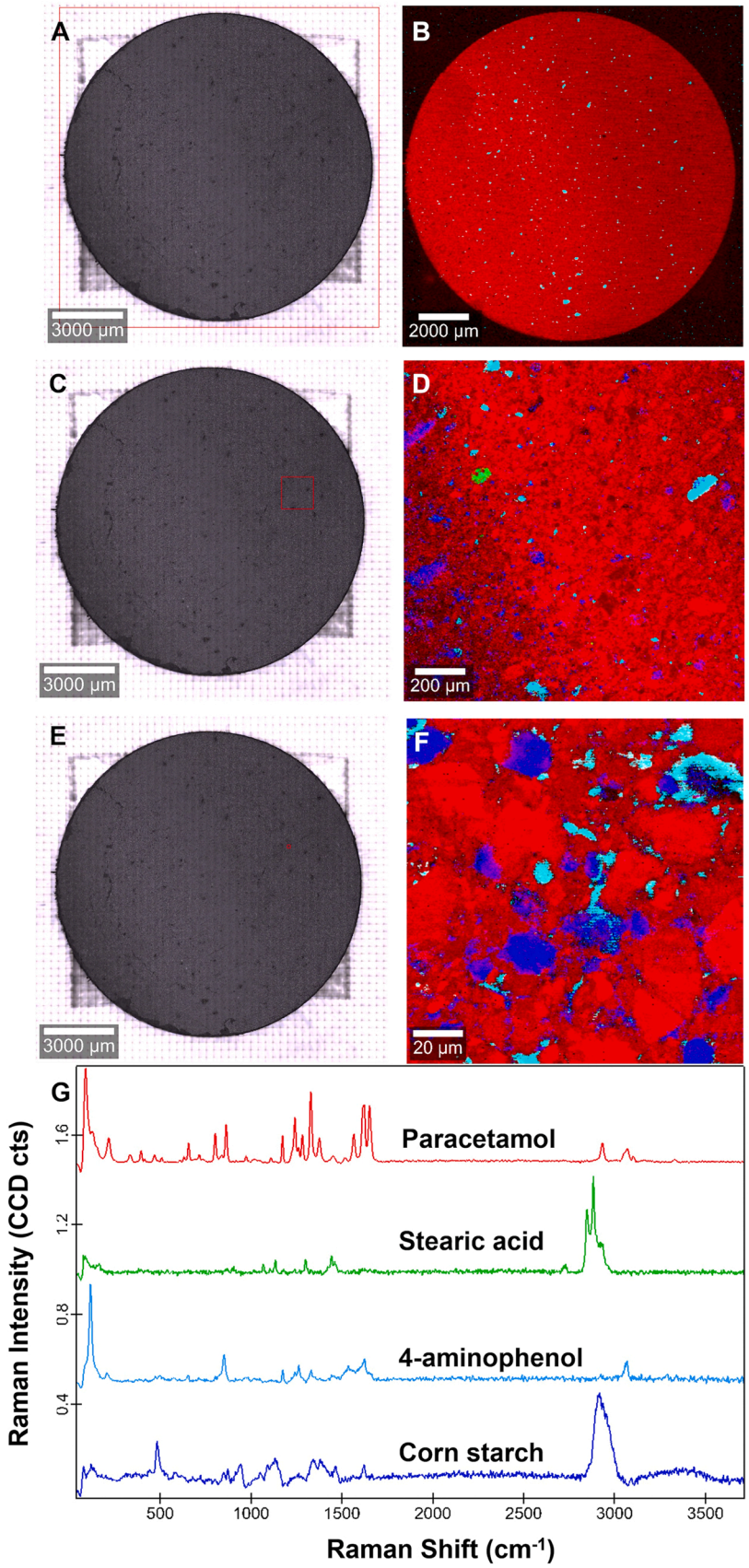

Fig. 3. Optical images of APAP-tablet with 10 % of 4-AP with the scan area marked in red for decreasing dimensions: 13.5 mm × 13.5 mm (A); 1.35 mm × 1.35 mm (C) and 135 µm x 135 µm (E) and the respective combined Rama image with 400 × 400 Raman spectra each image (B, D and F); Raman spectra used for the combined Raman image: 4-AP (cyan), APAP (red), stearic acid (green) and corn starch (blue) (G).

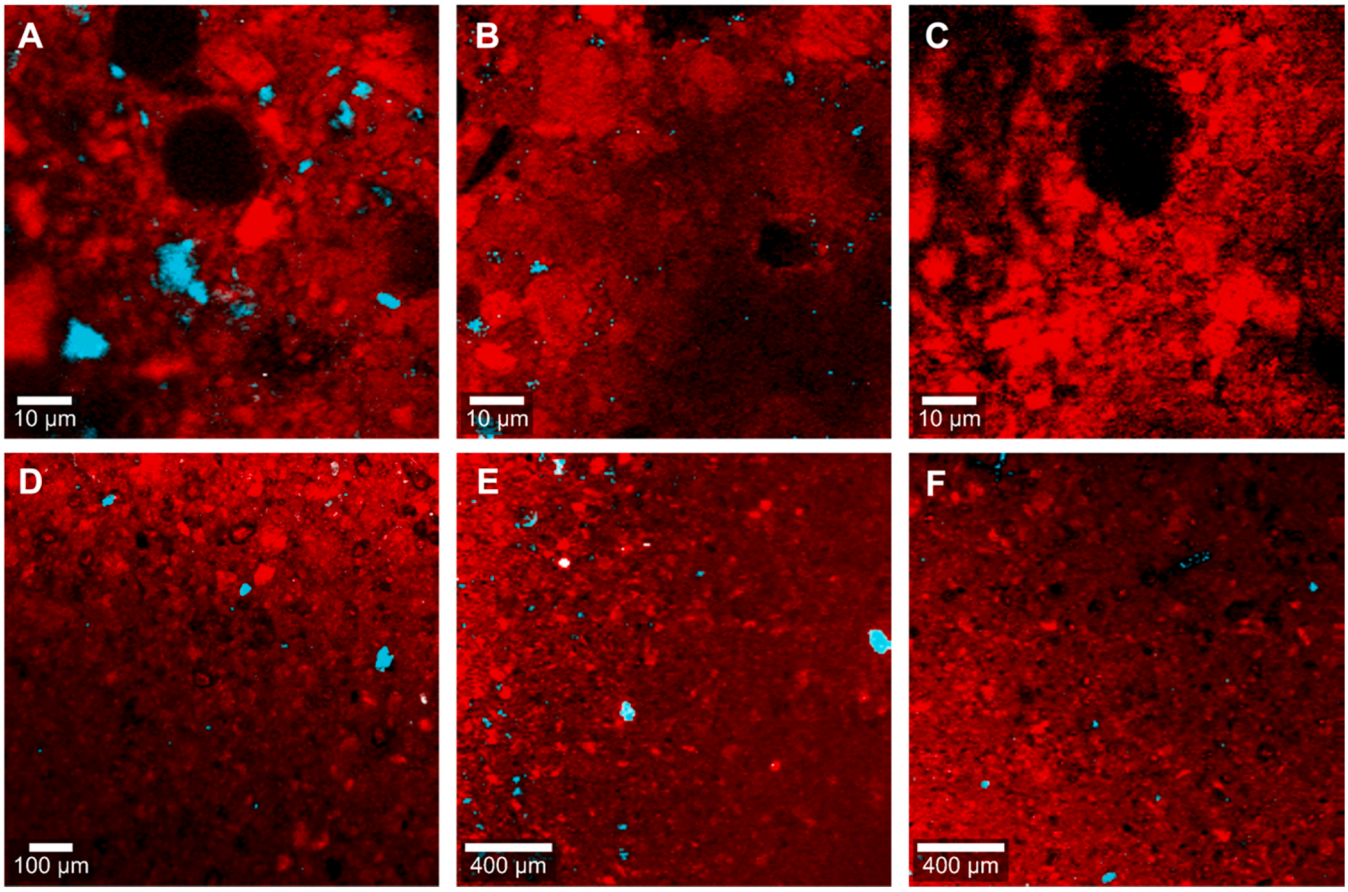

Fig. 4. Higher-resolution combined Raman images of APAP-tablets (80 µm x 80 µm; 40,000 Raman spectra) with variable 4-AP amounts: 10 % (A); 1 % (B); 0.5 % (C); Large combine Raman images of APAP-tablets with variable 4-AP amounts: 0.5 % (750 µm x 740 µm; 40,000 Raman spectra) (D); 0.1 % (2000 µm x 2000 µm; 40,000 Raman spectra) (E); 0.05 % (2000 µm x 2000 µm; 40,000 Raman spectra) (F).

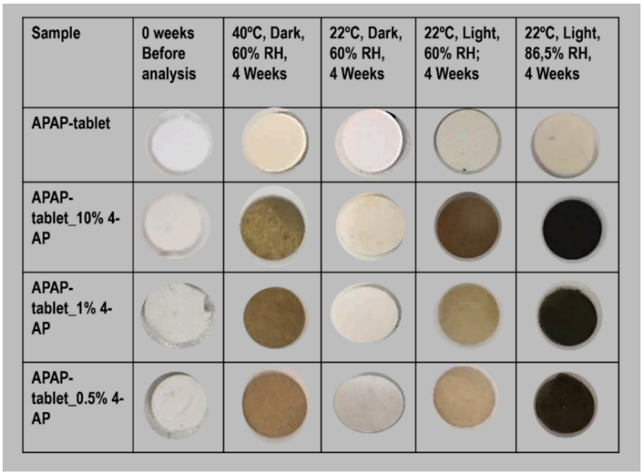

Fig. 5. Digital photographs of APAP-tablets and APAP-tablets with a variable amount of 4-AP (10 %, 1 %, 0.5 %) before and after submitted to 40ºC (Dark, 60 % RH), 22ºC (Dark, 60 % RH), 22ºC (Light, 60 % RH) and 22ºC (Light, 86.5 % RH).

To inquire about the sensitivity of Raman imaging to monitor variable amounts of 4-AP in the APAP-tablets, the contaminant 4-AP was spiked in the APAP-tablets for the following amounts: 0.05 %, 0.1 %, 0.5 %, 1 % and 10 % (w|w), and then analysed by confocal Raman microscopy. Fig. 4 presents the distribution of APAP (red colour) and 4-AP (cyan colour) over the APAP-tablets with variable amounts of 4-AP. In this case, corn-starch and stearic acid regions are not shown for sake of clarity.

Fig. 4A-C shows the high-resolution Raman images (80 µm x 80 µm, 40,000 Raman spectra), in which 4-AP was detected in the APAP-tablets for 1 % as the lowest amount of the contaminant. By increasing the scanned area to 2000 µm x 2000 µm (40,000 Raman spectra), 4-AP was detected in the APAP-tablet spiked at 0.05 % in the contaminant (cyan colour Fig. 4F). Although this percentage is still above the maximum allowed limit by Pharmacopoeias, which is 0.005 % in 4-AP, these results show the potential of the method to monitor the distribution of this contaminant in tablets [23,24].

Adequate storage and preservation of pharmaceutical formulations are fundamental factors for the effectiveness of API. To determine the chemical stability of a drug during storage, it is crucial to assess the effect of ambient conditions, such as temperature, relative humidity and light exposure. This type of study is described here for the first time, by using Raman imaging applied to APAP-tablets spiked with variable amounts of 4-AP (10 %, 1 % and 0.5 % w|w), which were subjected to different conditions of temperature, light and humidity over four weeks of shell-life. An APAP-tablet without 4-AP was used as an experiment control and thus subjected to similar conditions. Fig. 5 provides an illustrated summary of these experiments for the selected conditions. Note that the APAP-tablet and 4-AP spiked samples are initially colourless. Overall, the following main observations can be highlighted after a simple visual inspection of the samples. No significant colour changes were observed for the non-spiked APAP-tablets, confirming that light-protected APAP-tablets stored at room temperature and under dry conditions do not undergo visible changes in their characteristics [76]. All the tablets spiked with 4-AP, even for the lowest amount tested (0.5

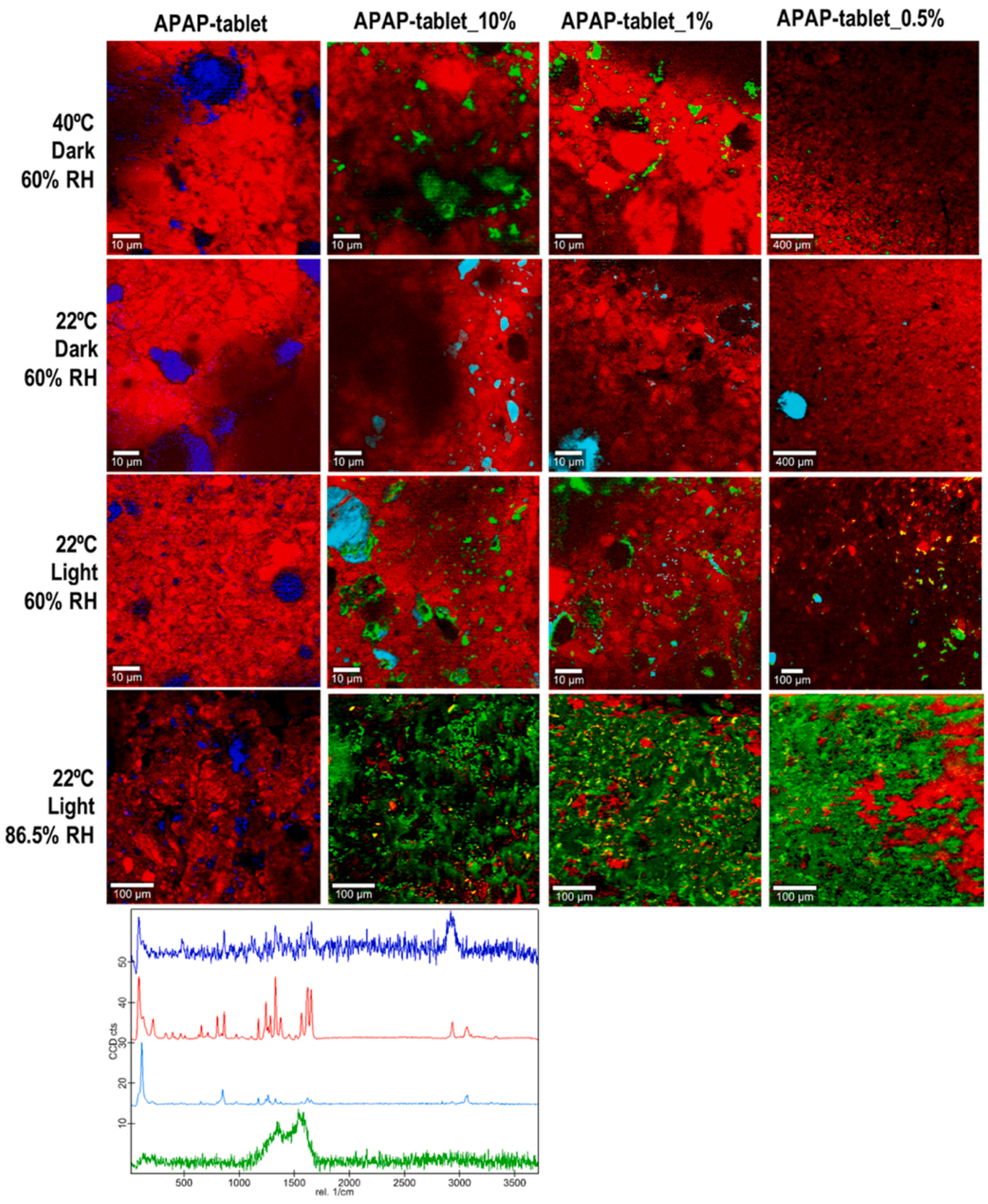

Fig. 6. High-resolution combined Raman images (80 µm x 80 µm; 40 000 Raman spectra) of APAP-tablet and APAP-tablets with variable 4-AP amounts 10 %, 1 % and large combined Raman images of APAP-tablets_0.5 % (2 000 µm x 2 000 µm, 40 000 Raman spectra or 750 µm x 750 µm; 40 000 Raman spectra) at 40ºC (Dark), 22ºC (Dark) and 22ºC (Light) after 4 weeks; Combined Raman images (500 µm x 500 µm; 40 000 Raman spectra) of APAP-tablet and APAP-tablets with variable 4-AP amounts exposed to 22º C with a relative humidity of 86.5 %. Raman spectra used for the combined Raman image: corn-starch (blue), APAP (red), 4-AP (cyan) and amorphous carbon (green).

%), exhibit colour changes at the surface, which are more pronounced after light exposure at 40ºC and, remarkably effective, in high moisture conditions. Note that all the contaminated tablets turned dark brown for 86,5 % RH. It has been reported that the oxidation of 4-AP produces p-benzoquinone monoimine, which slowly hydrolyses to p-benzoquinone or reacts with unoxidized 4-AP, giving a brown trinuclear dye (SI, Fig. S1) [77].

Based on the above results, selected samples were analysed by CRM, as depicted in Fig. 6.

In all experiments, the control APAP-tablet demonstrates the presence of APAP (red colour) and corn-starch (blue colour). Chemical products of degradation or hydrolysis reactions were not observed, namely hydroquinone, benzoquinone, 4-nitrophenol or 1,2,4-trihydroxybenzene [78]. This is in line with the reported stability of APAP as a stable API, when exposed to light, temperature (below 40ºC) and dry conditions during a period of four weeks. Indeed, the photochemical stability of APAP has already been reported by Sokół et al. [79], who have studied the influence of sunlight on the stability of APAP, and they have concluded that APAP is a non-photosensitive compound based on chromatographic data.

For the APAP-tablets contaminated with 4-AP, the tablets exposed to 22ºC in the dark show the presence of 4-AP (cyan colour) and APAP (red colour) in the Raman images after 4 weeks. This result is in line with the photographs in Fig. 5, in which no changes in the tablets' colour were observed.

On the other hand, the spiked tablets exposed to sunlight (22ºC) over four weeks exhibited light-brown colour (Fig. 5), which became more pronounced in the tablets with the highest load in 4-AP. This result suggests that the oxidation/degradation of 4-AP is activated by sunlight exposure. The Raman mappings of the APAP samples spiked with 4-AP exposed to sunlight (22ºC) revealed the presence of 4-AP (cyan colour) and amorphous carbon (green colour). Furthermore, the sample regions mapped as amorphous carbon are in the vicinity of 4-AP grains (Fig. 6), which seems consistent with photodegradation of the contaminant under laser irradiation. This result suggests that the brown compound formed by light irradiation is very sensitive to the laser used in the Raman image acquisition, and the presence of amorphous carbon is an effect of its degradation. We have decreased the laser power but, in these conditions, there is significant decrease of the equipment's sensitivity, and no Raman signal was observed.

Rather than a limitation, this observation can be an indirect way to map regions in the tablet sample enriched in the photosensitive 4-AP contaminant. As Fig. 6 shows, the 4-AP photodegradation is more extensive in conditions of high temperature (40ºC) and 86.5 % relative humidity. In these conditions, the Raman images of the APAP-tablets contaminated with 4-AP show a layer of amorphous carbon (green colour) as the most distinctive feature, which supports the above interpretation.

ATR-FTIR was used to analyse the APAP-tablets with 10 % of 4-AP before and after exposure to 86.5 % relative humidity to get information about the 4-AP oxidation/degradation (Fig. S2). The FTIR spectra of APAP-tablet and 4-AP are also demonstrated for comparison. First, we did not observe the 4-AP on the APAP-tablets_10 % (see grey shadows in Fig. S2); only APAP was observed. Second, the APAP-tablet_10 % exposed to 86.5 % relative humidity did not demonstrate any additional bands that could explain the changes in the tablet colour (black colour).

Thus, our finding opens up future studies on using this photochemical process for Raman image probing of 4-AP in pharmaceutic products.

4. Conclusion

In conclusion, Raman imaging has been demonstrated as a valuable tool for getting information on the distribution and homogeneity of the API and excipients present on APAP pharmaceutical tablets. By carefully inspecting APAP-tablet Raman maps, it was possible to identify the API and the two main excipients (corn-starch and stearic acid) and observe the dimension/size of the respective grains.

For the first time, it was demonstrated that 4-AP in APAP-tablets can be detected as low as 0.05 % w|w, by using Raman images of laboratorial spiked samples. This result is auspicious because non-destructive quality control practices can be developed, which include Raman measurements performed in the factory assembly.

Unlike the pure APAP-tablets, samples contaminated with 4-AP suffer chemical degradation, which confers brown colouration to the tablets and result in *a* photosensitive 4-AP contaminant (amorphous carbon) detected in the Raman maps. This degradation process was more pronounced for samples having a higher amount of 4-AP, at higher temperatures and high relative humidity.

CRediT authorship contribution statement

Sara Fateixa: Research planning, Methodology, Supervision, Writing – original draft, Writing – review & editing. **Otílio Mulandeza:** Investigation. **Helena I.S. Nogueira:** Supervision, Writing – review & editing. **Tito Trindade:** General scientific guidance, Writing – review & editing.

All authors have given approval for the final version of the manuscript.

Declaration of Competing Interest

The authors declare that they have no known competing financial interests or personal relationships that could have appeared to influence the work reported in this paper.

Data Availability

Data will be made available on request.

Acknowledgement

This work was developed within the scope of the project CICECO-Aveiro Institute of Materials, UIDB/50011/2020, UIDP/50011/2020 & LA/P/0006/2020, financed by national funds through the FCT/MCTES (PIDDAC) and when appropriate cofinanced by FEDER under the PT2020 Partnership Agreement. S. F. thanks FCT for her research contract (REF-069–88-ARH-2018), which is funded by national funds (OE), through FCT-Fundaçaõ para a Ciência e a Tecnologia, I.P., in the scope of the framework contract foreseen in the numbers 4, 5, and 6 of the article 23, of the Decree-Law 57/2016, of August 29, changed by Law 57/2017, of July 19.

Appendix A. Supporting information

Supplementary data associated with this article can be found in the online version at doi:10.1016/j.vibspec.2022.103488.

References

[1] R.M. Haleem, M.Y. Salem, F.A. Fatahallah, L.E. Abdelfattah, Quality in the pharmaceutical industry - a literature review, Saudi Pharm. J. 23 (2015) 463–469, https://doi.org/10.1016/j.jsps.2013.11.004.

[2] L. Teklu, E. Adugna, A. Ashenef, Quality evaluation of paracetamol tablets obtained from the common shops (Kiosks) in Addis Ababa, Ethiopia, Int. J. Pharm. Sci. Res. 5 (2014) 3502–3510.

[3] N. Nasrin, F. Rizwan, M. Asaduzzaman, R. Mowla, A. Alam, A comparative study of physical parameters of selected ketorolac tromethamine tablets available in the pharma market of Bangladesh, J. Appl. Pharm. Sci. (2011) (2011) 101–103, www.en.wikipedia.org, (accessed November 9, 2021).

[4] M. Sardella, G. Belcher, C. Lungu, T. Ignoni, M. Camisa, D.I. Stenver, P. Porcelli, M. D'Antuono, N.G. Castiglione, A. Adams, G. Furlan, I. Grisoni, S. Hall, L. Boga, V. Mancini, M. Ciuca, D. Chonzi, B. Edwards, A.A. Mangoni, M. Tuccori, E. Prokofyeva, F. De Gregorio, M. Bertazzoli Grabinski Broglio, B. van Leeuwen, P. Kruger, C. Rausch, H. Le Louet, Monitoring the manufacturing and quality of medicines: a fundamental task of pharmacovigilance, 204209862110384, Ther. Adv. Drug Saf. 12 (2021), https://doi.org/10.1177/20420986211038436.

[5] World Health Organization, Qual. Assur. Pharm.: a Compend. Guidel. Relat. Mater. (2007), https://doi.org/10.1590/s1516-93322007000400026.

[6] A. Johnston, D.W. Holt, T. London, Substandard drugs: a potential crisis for public health correspondence, Br. J. Clin. Pharm. 78 (2013) 218–243, https://doi.org/10.1111/bcp.12298.

[7] P.N. Newton, M.D. Green, F.M. Fernández, Impact of poor-quality medicines in the "developing" world, Trends Pharm. Sci. 31 (2010) 99–101, https://doi.org/10.1016/j.tips.2009.11.005.

[8] B.L. Gbenga, Y. Taiwo, Studies of the effect of storage conditions on some pharmaceutical parameters of powders and tablets, Dhaka University, J. Pharm. Sci. 14 (2015) 147–151.

[9] C. Ammann, Stability studies needed to define the handling and transport conditions of sensitive pharmaceutical or biotechnological products, AAPS Pharm. Sci. Tech. 12 (2011) 1264–1275, https://doi.org/10.1208/s12249-011-9684-0.

[10] N. Kumar, A. Jha, Temperature excursion management: a novel approach of quality system in pharmaceutical industry, Saudi Pharm. J. 25 (2017) 176–183, https://doi.org/10.1016/j.jsps.2016.07.001.

[11] A. Alqurshi, Household storage of pharmaceutical products in Saudi Arabia; a call for utilising smart packaging solutions, Saudi Pharm. J. 28 (2020) 1411–1419, https://doi.org/10.1016/j.jsps.2020.09.006.

[12] S. Yoshioka, Chemical stability of drug substances, in: Stability of Drugs and Dosage Forms, Kluwer Academic Publishers, 2002, pp. 3–137, https://doi.org/10.1007/0-306-46829-8_2.

[13] K.C. Waterman, R.C. Adami, K.M. Alsante, A.S. Antipas, D.R. Arenson, R. Carrier, J. Hong, M.S. Landis, F. Lombardo, J.C. Shah, E. Shalaev, S.W. Smith, H. Wang, Hydrolysis in pharmaceutical formulations, Pharm. Dev. Technol. 7 (2002) 113–146, https://doi.org/10.1081/PDT-120003494.

[14] D.A. Comely, J.A. Ritter, N-acetyl-p-aminophenol (tylenol elixir) as a pediatric antipyretic-analgesic, J. Am. Med Assoc. 160 (1956) 1219–1221, https://doi.org/10.1001/jama.1956.02960490033009.

[15] T.R. Ferreira, S.B. Filho, A.F. Borgatto, L.C. Lopes, Analgésicos, antipiréticos e anti-inflamatórios não esteroides em prescrições pediátricas, Cienc. e Saude Coletiva. 18 (2013) 3695–3704, https://doi.org/10.1590/S1413-81232013001200025.

[16] S. Mehretie, S. Admassie, T. Hunde, M. Tessema, T. Solomon, Simultaneous determination of N-acetyl-p-aminophenol and p-aminophenol with poly(3,4-ethylenedioxythiophene) modified glassy carbon electrode, Talanta 85 (2011) 1376–1382, https://doi.org/10.1016/j.talanta.2011.06.019.

[17] K. Brune, H.U. Zeilhofer, Antipyretic analgesics, in: Handbook of Pain Management: A Clinical Companion to Textbook of Pain, Elsevier Inc.,, 2003, pp. 341–351, https://doi.org/10.1016/B978-0-443-07201-7.50026-6.

[18] M. de Martino, A. Chiarugi, Recent advances in pediatric use of oral paracetamol in fever and pain management, Pain. Ther. 4 (2015) 149–168, https://doi.org/10.1007/s40122-015-0040-z.

[19] U.B.R. Khandavilli, L. Keshavarz, E. Skořepová, R.R.E. Steendam, P.J. Frawley, Organic salts of pharmaceutical impurity p-Aminophenol, Molecules 25 (2020) 1910, https://doi.org/10.3390/molecules25081910.

[20] A. Mujahid, Y. Ali, A. Afzal, T. Hussain, A. Tufail Shah, K. Shehzad, M. Umar Farooq, Rapid assay of the comparative degradation of acetaminophen in binary and ternary combinations, Arab. J. Chem. 7 (2014) 522–524, https://doi.org/10.1016/j.arabjc.2012.10.014.

[21] A. Yesilada, H. Erdogan, M. Ertan, Second derivative spectrophotometric determination of p-aminophenol in the presence of paracetamol, Anal. Lett. 24 (1991) 129–138, https://doi.org/10.1080/00032719108052889.

[22] J. Forshed, F.O. Andersson, S.P. Jacobsson, NMR and Bayesian regularized neural network regression for impurity determination of 4-aminophenol, J. Pharm. Biomed. Anal. 29 (2002) 495–505, https://doi.org/10.1016/S0731-7085(02)00086-9.

[23] Council of Europe; European Pharmacopoeia Commission., European pharmacopoeia. (Book, 2007) [WorldCat.org], Strasbourg: Council Of Europe, 2007., 2007.

[24] M.S. Bloomfield, A sensitive and rapid assay for 4-aminophenol in paracetamol drug and tablet formulation, by flow injection analysis with spectrophotometric detection, in: Talanta, Elsevier, 2002, pp. 1301–1310, https://doi.org/10.1016/S0039-9140(02)00421-6.

[25] F.A. Mohamed, M.A. AbdAllah, S.M. Shammat, Selective spectrophotometric determination of p-aminophenol and acetaminophen, Talanta 44 (1997) 61–68, https://doi.org/10.1016/S0039-9140(96)02013-9.

[26] I.I. Hewala, High-performance liquid chromatographic and derivative difference spectrophotometric methods for the determination of acetaminophen and its degradation product in aged pharmaceutical formulations, Anal. Lett. 27 (1994) 561–582, https://doi.org/10.1080/00032719408001095.

[27] L. Monser, F. Darghouth, Simultaneous LC determination of paracetamol and related compounds in pharmaceutical formulations using a carbon-based column, J. Pharm. Biomed. Anal. 27 (2002) 851–860, https://doi.org/10.1016/S0731-7085(01)00515-5.

[28] E. Wyszecka-Kaszuba, M. Warowna-Grześkiewicz, Z. Fijałek, in: J. Pharm Biomed Anal (Ed.), Determination of 4-aminophenol impurities in multicomponent analgesic preparations by HPLC with amperometric detection, Elsevier, 2003, pp. 1081–1086, https://doi.org/10.1016/S0731-7085(03)00212-7.

[29] A. Marín, C. Barbas, LC/MS for the degradation profiling of cough-cold products under forced conditions, J. Pharm. Biomed. Anal. 35 (2004) 1035–1045, https://doi.org/10.1016/j.jpba.2004.03.011.

[30] K.D. Altria, N.G. Clayton, M. Hart, R.C. Harden, J. Hevizi, J.V. Makwana, M. J. Portsmouth, An inter-company cross-validation exercise on capillary electrophoresis testing of dose uniformity of paracetamol content in formulations, Chromatographia 39 (1994) 180–184, https://doi.org/10.1007/BF02274498.

[31] G. Chen, J. Ye, H. Bao, P. Yang, Determination of the rate constants and activation energy of acetaminophen hydrolysis by capillary electrophoresis, J. Pharm. Biomed. Anal. 29 (2002) 843–850, https://doi.org/10.1016/S0731-7085(02)00211-X.

[32] S. Boonkerd, M. Lauwers, M.R. Detaevernier, Y. Michotte, Sep. simultaneous Determ. Compon. Analg. Table Formul. micellar Electrokinet. Chromatogr. (1995).

[33] L. Suntornsuk, O. Pipitharome, P. Wilairat, Simultaneous determination of paracetamol and chlorpheniramine maleate by micellar electrokinetic chromatography, J. Pharm. Biomed. Anal. 33 (2003) 441–449, https://doi.org/10.1016/S0731-7085(03)00288-7.

[34] N. Wang, H. Cao, L. Wang, F. Ren, Q. Zeng, X. Xu, J. Liang, Y. Zhan, X. Chen, Recent advances in spontaneous raman spectroscopic imaging: instrumentation and applications, Curr. Med Chem. 27 (2019) 6188–6207, https://doi.org/10.2174/0929867326666190619114431.

[35] A. Rzhevskii, The recent advances in raman microscopy and imaging techniques for biosensors, Biosens. (Basel) 9 (2019), https://doi.org/10.3390/bios9010025.

[36] H. Eksi-Kocak, S. Ilbasmis Tamer, S. Yilmaz, M. Eryilmaz, I.H. Boyaci, U. Tamer, Quantification and spatial distribution of salicylic acid in film tablets using FT-Raman mapping with multivariate curve resolution, Asian J. Pharm. Sci. 13 (2018) 155–162, https://doi.org/10.1016/j.ajps.2017.07.010.

[37] S.C. Brown, M. Claybourn, D. Sievwright, V. Fearnside, C. Ashman, Lean Raman imaging for rapid assessment of homogeneity in pharmaceutical formulations, Appl. Spectrosc. 64 (2010) 442–447, https://doi.org/10.1366/000370210791114239.

[38] S. Šašić, S. Mehrens, Raman chemical mapping of low-content active pharmaceutical ingredient formulations. iii. statistically optimized sampling and detection of polymorphic forms in tablets on stability, Anal. Chem. 84 (2012) 1019–1025, https://doi.org/10.1021/ac202396u.

[39] H. Carruthers, D. Clark, F. Clarke, K. Faulds, D. Graham, Comparison of Raman and near-infrared chemical mapping for the analysis of pharmaceutical tablets, Appl. Spectrosc. 75 (2021) 178–188, https://doi.org/10.1177/0003702820952440.

[40] T. Čapková, T. Pekárek, B. Hanulíková, P. Matějka, Application of reverse engineering in the field of pharmaceutical tablets using Raman mapping and chemometrics, J. Pharm. Biomed. Anal. 209 (2022), 114496, https://doi.org/10.1016/j.jpba.2021.114496.

[41] H. Carruthers, D. Clark, F. Clarke, K. Faulds, D. Graham, Comparison of Raman and near-infrared chemical mapping for the analysis of pharmaceutical tablets, Appl. Spectrosc. 75 (2021) 178–188, https://doi.org/10.1177/0003702820952440.

[42] D.L. Galata, B. Zsiros, L.A. Mészáros, B. Nagy, E. Szabó, A. Farkas, Z.K. Nagy, Raman mapping-based non-destructive dissolution prediction of sustained-release tablets, J. Pharm. Biomed. Anal. 212 (2022), 114661, https://doi.org/10.1016/j.jpba.2022.114661.

[43] C. Vogel, C. Adam, D. McNaughton, Determination of phosphate phases in sewage sludge ash-based fertilizers by Raman microspectroscopy, Appl. Spectrosc. 67 (2013) 1101–1105, https://doi.org/10.1366/12-06955/ASSET/IMAGES/LARGE/10.1366_12-06955-FIG1.JPEG.

[44] P.C. Pinheiro, S. Fateixa, H.I.S. Nogueira, T. Trindade, Magnetite-supported gold nanostars for the Uptake and SERS detection of tetracycline, 31. 9 (2018) 31, Nanomaterials Vol. 9 (2019), https://doi.org/10.3390/NANO9010031.

[45] M. Tian, C.L.M. Morais, H. Shen, W. Pang, L. Xu, Q. Huang, F.L. Martin, Direct identification and visualisation of real-world contaminating microplastics using Raman spectral mapping with multivariate curve resolution-alternating least squares, J. Hazard Mater. 422 (2022), 126892, https://doi.org/10.1016/J.JHAZMAT.2021.126892.

[46] T. Yaseen, D.W. Sun, J.H. Cheng, Raman imaging for food quality and safety evaluation: fundamentals and applications, Trends Food Sci. Technol. 62 (2017) 177–189, https://doi.org/10.1016/J.TIFS.2017.01.012.

[47] M. Jermyn, J. Desroches, K. Aubertin, K. St-Arnaud, W.-J. Madore, E. de Montigny, M.-C. Guiot, D. Trudel, B.C. Wilson, K. Petrecca, F. Leblond, A review of Raman spectroscopy advances with an emphasis on clinical translation challenges in oncology, Phys. Med Biol. 61 (2016) R370–R400, https://doi.org/10.1088/0031-9155/61/23/R370.

[48] C.W. Freudiger, W. Min, B.G. Saar, S. Lu, G.R. Holtom, C. He, J.C. Tsai, J.X. Kang, X.S. Xie, Label-free biomedical imaging with high sensitivity by stimulated raman scattering microscopy, Science 322 (2008) (1979) 1857–1861, https://doi.org/10.1126/science.1165758.

[49] Z. Ling, A. Wang, Spatial distributions of secondary minerals in the Martian meteorite MIL 03346,168 determined by Raman spectroscopic imaging, J. Geophys Res Planets 120 (2015) 1141–1159, https://doi.org/10.1002/2015JE004805.

[50] D. Lauwers, P. Brondeel, L. Moens, P. Vandenabeele, situ raman Mapp. Art. Objects, Philos. Trans. R. Soc. A: Math., Phys. Eng. Sci. 374 (2016), https://doi.org/10.1098/RSTA.2016.0039.

[51] F.D.S.L. Borba, T. Jawhari, R. Saldanha Honorato, A. de Juan, Confocal Raman imaging and chemometrics applied to solve forensic document examination involving crossed lines and obliteration cases by a depth profiling study, Analyst 142 (2017) 1106–1118, https://doi.org/10.1039/C6AN02340A.

[52] S. Deng, L. Liu, Z. Liu, Z. Shen, G. Li, Y. He, Line-scanning Raman imaging spectroscopy for detection of fingerprints, Appl. Opt. Vol. 51 (Issue 17) (2012) 3701–3706, https://doi.org/10.1364/AO.51.003701.

[53] K.C. Gordon, C.M. McGoverin, Raman mapping of pharmaceuticals, Int J. Pharm. 417 (2011) 151–162, https://doi.org/10.1016/j.ijpharm.2010.12.030.

[54] D.S. Hausman, R.T. Cambron, A. Sakr, Application of Raman spectroscopy for on-line monitoring of low dose blend uniformity, Int J. Pharm. 298 (2005) 80–90, https://doi.org/10.1016/j.ijpharm.2005.04.011.

[55] M.J. Henson, L. Zhang, Drug characterization in low dosage pharmaceutical tablets using Raman microscopic mapping, Appl. Spectrosc. 60 (2006) 1247–1255, https://doi.org/10.1366/000370206778998987.
[56] E. Widjaja, R.K.H. Seah, Application of Raman microscopy and band-target entropy minimization to identify minor components in model pharmaceutical tablets, J. Pharm. Biomed. Anal. 46 (2008) 274–281, https://doi.org/10.1016/j.jpba.2007.09.023.
[57] S. Šašić, Raman mapping of low-content API pharmaceutical formulations. I. Mapping of alprazolam in Alprazolam/Xanax tablets, Pharm. Res 24 (2007) 58–65, https://doi.org/10.1007/s11095-006-9118-y.
[58] H. Nie, Z. Liu, B.C. Marks, L.S. Taylor, S.R. Byrn, P.J. Marsac, Analytical approaches to investigate salt disproportionation in tablet matrices by Raman spectroscopy and Raman mapping, J. Pharm. Biomed. Anal. 118 (2016) 328–337, https://doi.org/10.1016/j.jpba.2015.10.024.
[59] C.F. Marques, S.M. Olhero, P.M.C. Torres, J.C.C. Abrantes, S. Fateixa, H.I. S. Nogueira, I.A.C. Ribeiro, A. Bettencourt, A. Sousa, P.L. Granja, J.M.F. Ferreira, Novel sintering-free scaffolds obtained by additive manufacturing for concurrent bone regeneration and drug delivery: Proof of concept, Mater. Sci. Eng. C. 94 (2019), https://doi.org/10.1016/j.msec.2018.09.050.
[60] L. Menilli, A.R. Monteiro, S. Lazzarotto, F.M.P. Morais, A.T.P.C. Gomes, N.M. M. Moura, S. Fateixa, M.A.F. Faustino, M.G.P.M.S. Neves, T. Trindade, G. Miolo, Graphene oxide and graphene quantum dots as delivery systems of cationic porphyrins: photo-antiproliferative activity evaluation towards T24 human bladder cancer cells, Pharmaceutics 13 (2021) 1512, https://doi.org/10.3390/pharmaceutics13091512.
[61] A.R. Monteiro, C.I.V. Ramos, S. Fateixa, N.M.M. Moura, M.G.P.M.S. Neves, T. Trindade, Hybrids based on graphene oxide and porphyrin as tools for detection and stabilization of DNA G-quadruplexes, ACS Omega 3 (2018) 11184–11191, https://doi.org/10.1021/acsomega.8b01366.
[62] Â. Semitela, S. Carvalho, C. Fernandes, S. Pinto, S. Fateixa, H.I.S. Nogueira, I. Bdikin, A. Completo, P.A.A.P. Marques, G. Gonçalves, Biomimetic graphene/spongin scaffolds for improved osteoblasts bioactivity via dynamic mechanical stimulation, Macromol. Biosci. 22 (2022), 2100311, https://doi.org/10.1002/mabi.202100311.
[63] S. Fateixa, H.I.S. Nogueira, T. Trindade, Carbamazepine polymorphism: a re-visitation using Raman imaging, Int J. Pharm. 617 (2022), 121632, https://doi.org/10.1016/j.ijpharm.2022.121632.
[64] S. Fateixa, H.I.S. Nogueira, J.A. Paixão, R. Fausto, T. Trindade, Insightful vibrational imaging study on the hydration mechanism of carbamazepine, Phys. Chem. Chem. Phys. 24 (2022) 19502–19511, https://doi.org/10.1039/D2CP02185D.
[65] H. Carruthers, D. Clark, F.C. Clarke, K. Faulds, D. Graham, Evaluation of laser direct infrared imaging for rapid analysis of pharmaceutical tablets, Anal. Methods 14 (2022) 1862–1871, https://doi.org/10.1039/D2AY00471B.
[66] B.N. Khlebtsov, D.N. Bratashov, N.G. Khlebtsov, Tip-functionalized Au@Ag nanorods as ultrabright surface-enhanced Raman scattering probes for bioimaging in off-resonance mode, J. Phys. Chem. C. 122 (2018) 17983–17993, https://doi.org/10.1021/acs.jpcc.8b04772.
[67] J.B. Nanubolu, J.C. Burley, Investigating the recrystallization behavior of amorphous paracetamol by variable temperature Raman studies and surface Raman mapping, Mol. Pharm. 9 (2012) 1544–1558, https://doi.org/10.1021/mp300035g.
[68] J.F. Kauffman, L.M. Batykefer, D.D. Tuschel, Raman detected differential scanning calorimetry of polymorphic transformations in acetaminophen, J. Pharm. Biomed. Anal. 48 (2008) 1310–1315, https://doi.org/10.1016/j.jpba.2008.09.008.
[69] K. Kachrimanis, D.E. Braun, U.J. Griesser, Quantitative analysis of paracetamol polymorphs in powder mixtures by FT-Raman spectroscopy and PLS regression, J. Pharm. Biomed. Anal. 43 (2007) 407–412, https://doi.org/10.1016/j.jpba.2006.07.032.
[70] C. Li, D. Zhang, M.N. Slipchenko, J.X. Cheng, Mid-infrared photothermal imaging of active pharmaceutical ingredients at submicrometer spatial resolution, Anal. Chem. 89 (2017) 4863–4867, https://doi.org/10.1021/acs.analchem.6b04638.
[71] M. Ramos de Almeida, K. de Sá Oliveira, R. Stephani, L. Fernando Cappa de Oliveira, Application of FT-Raman spectroscopy and chemometric analysis for determination of adulteration in milk powder, Anal. Lett. 45 (2012) 2589–2602, https://doi.org/10.1080/00032719.2012.698672.
[72] A.M. Amado, C. Azevedo, P.J.A. Ribeiro-Claro, Conformational and vibrational reassessment of solid paracetamol, Spectrochim. Acta A Mol. Biomol. Spectrosc. 183 (2017) 431–438, https://doi.org/10.1016/j.saa.2017.04.076.
[73] M.A. Elbagerma, H.G.M. Edwards, T. Munshi, I.J. Scowen, Identification of a new cocrystal of citric acid and paracetamol of pharmaceutical relevance, CrystEngComm 13 (2011) 1877–1884, https://doi.org/10.1039/c0ce00461h.
[74] S. Sobanska, J. Barbillat, M. Moreau, N. Nuns, I. de Waele, D. Petitprez, Y. Tobon, C. Brémard, Influence of stearic acid coating of the NaCl surface on the reactivity with NO2 under humidity, Phys. Chem. Chem. Phys. 17 (2015) 10963–10977, https://doi.org/10.1039/c4cp05655h.
[75] W.P. Griffith, T.Y. Koh, Vibrational spectra of 1,2-benzenedithiol, 2-aminothiophenol and 2-aminophenol and their SER spectra, Spectrochim. Acta A Mol. Biomol. Spectrosc. 51 (1995) 253–267, https://doi.org/10.1016/0584-8539(94)E0086-P.
[76] W.H.O. Annex, 3 WHO good Manuf. Pract. Pharm. Prod.: Main. Princ. (2011).
[77] M.A. Lieber, 2 Final Report on the Safety Assessment of p-Aminophenol, m-Aminophenol, and o-Aminophenol | Enhanced Reader, J Am Coll Toxicol. (1988) 278. moz-extension://a33bee57–7906-d44c-907d-3a913fbc922b/enhanced-reader.html?openApp&pdf=https%3A%2F%2Fjournals.sagepub.com%2Fdoi%2Fpdf%2F10.3109%2F10915818809023134 (accessed January 6, 2022).
[78] N. Jallouli, K. Elghniji, H. Trabelsi, M. Ksibi, Photocatalytic degradation of paracetamol on TiO2 nanoparticles and TiO2/cellulosic fiber under UV and sunlight irradiation, Arab. J. Chem. 10 (2017) S3640–S3645, https://doi.org/10.1016/j.arabjc.2014.03.014.
[79] A. Sokół, K. Borowska, J. Karpińska, Investigating the influence of some environmental factors on the stability of paracetamol, naproxen, and diclofenac in simulated natural conditions, Pol. J. Environ. Stud. 26 (2017) 293–302, https://doi.org/10.15244/pjoes/64310.